

**Evaluation of stress distribution patterns on short  
implants with differing crown heights: A Three  
Dimensional Finite Element Analysis**

A THESIS  
SUBMITTED TO THE FACULTY OF THE GRADUATE SCHOOL  
OF THE UNIVERSITY OF MINNESOTA  
BY

Tanawat Ritkajorn, D.D.S.

IN PARTIAL FULFILLMENT OF THE REQUIREMENTS  
FOR THE DEGREE OF  
MASTER OF SCIENCE

Alex S. L. Fok, PhD.

December 2010



## **Acknowledgments**

I would like to thank my principal advisor Dr. Alex S. L. Fok, Director of the Dental Research Center for Biomaterials and Biomechanics, School of Dentistry, University of Minnesota, for providing me with this invaluable experience in biomechanical research methodology and for allowing me access to the facilities. To the best fellow I have met thus far, Jianying Li, Ph.D., I am ever so grateful for his wise counsel and his patience in guiding me, a novice in biomechanics and finite element analysis research. I would also like to thank Dr. Andrea Hsu for her gracious advice and the proofreading of this thesis.

My deepest gratitude to my Program Director, Dr. James R. Holtan, Graduate Prosthodontic Program Director, University of Minnesota, School of Dentistry, for instigating in me this drive to excel throughout my residency training and for supporting my research. Above all, I am thankful to my co-director, Dr. John K. Schulte, for being the inspiration of this short implant research and a steppingstone in my implant prosthodontic education.

## **Dedication**

To my parents, Suranart and Pradab Ritkajorn, and my aunt, Supun Karkjanakeyoon, for their unconditional love and support.

I am grateful for everything they have done to support our family. It is their unfaltering faith, encouragement, and generous financial contribution that allowed me to pursue my education in the United States. This work is a reflection of these exceptional human beings whom I have the honor of calling parents.

## Abstract

**Statement of problem:** The use of short dental implants is usually confined to areas of the mouth with limited vertical bone height. As a result, longer implant crowns are required to restore the occlusion with the opposing arch, leading to a disproportionate crown-to-implant ratio (C/I ratio).

**Purpose:** The purpose of this study was to evaluate the stress distribution patterns on crestal bone of short implants plateau-designed connected with different crown heights, and to compare these findings with those of regular implants.

**Material and Methods:** Two implant designs ( $\varnothing 5$  mm $\times$ 6 mm and  $\varnothing 5$  mm $\times$ 11 mm) and abutments ( $\varnothing 5$  mm $\times$ 9 mm and  $\varnothing 5$  mm $\times$ 5 mm) were scanned using a micro-CT scanner. STL surface models were subsequently extracted to generate surfaces. All models were imported to Abaqus CAE for three-dimensional non-linear finite element analysis. For each implant model, loadings of 100, 200, and 700 N were simulated in 2 directions: pure vertical and at an oblique angle of 15 degrees.

**Results:** At 100 and 200 N oblique loads, peak compressive and tensile stresses ranged from 18.30 to 53.57 MPa and 7.39 to 43.95 MPa, respectively. At 700 N oblique loads, the  $\varnothing 5$  mm $\times$ 6 mm implant with long abutment model exceeded the compressive and tensile strength of cortical bone, at 193.4 and 158.6 MPa correspondingly. For 700 N oblique loads, increasing crown height increased peak compressive stress by 28.6 % and peak tensile stress by 28.4 %. Stress distribution patterns showed the highest amounts of stress located at the implant crest module in cortical bone.

**Conclusion:** Stress distribution patterns for the oblique loads of 100 and 200 N were similar in all models, regardless of the C/I ratios. All peak stresses were within physiological tolerance. At 700 N loads, increasing crown height resulted in bone failure.

**Table of Contents**

Acknowledgments	i
Dedication	ii
Abstract	iii
Table of contents	iv
List of Tables	vi
List of Figures	vii
Chapter I Introduction	1
Objectives	3
Hypothesis	3
Keywords	4
Limitation	4
Benefit of study	4
Chapter II Literature Review	
The use and survival of short dental implants	5
Crown-to-implant ratios	8
Crestal bone loss and stress distribution	10
Finite element analysis	11
Chapter III Material and Methods	16
Chapter IV Results	23
Chapter V Discussion and Conclusion	37

Conclusion	42 <sup>v</sup>
Clinical implication	42
Bibliography	43

**List of Tables**

Table 1 Young's Modulus and Poisson's Ratio of Materials Used	19
Table 2 Number of elements and nodes used in FE Models	21
Table 3 Maximum Compressive Stress of all models under oblique loads of 700 N	24
Table 4 Maximum Tensile Stress of all models under oblique loads of 700 N	28
Table 5 Maximum Compressive Stress of all models under vertical loads of 700 N	32
Table 6 Maximum Tensile Stress of all models under vertical loads of 700 N	33

**List of Figures**

Figure 1. Implant and Abutment Geometry	17
Figure 2. Measurement of models	18
Figure 3. Implant-bone models	20
Figure 4. Maximum Compressive Stress in all models.	23
Figure 5. Minimum Principal Stress on Model A under oblique loads of 200 N	24
Figure 6. Minimum Principal Stress on Model B under oblique loads of 200 N	25
Figure 7. Minimum Principal Stress on Model C under oblique loads of 200 N	25
Figure 8. Minimum Principal Stress on Model D under oblique loads of 200 N	26
Figure 9. Minimum Principal Stress distribution pattern in Model B under oblique loads of 200 N	27
Figure 10 Maximum Tensile Stress in all models.	28
Figure 11 Maximum Principal Stress on Model A under oblique loads of 200 N	29
Figure 12 Maximum Principal Stress on Model B under oblique loads of 200 N	29
Figure 13 Maximum Principal Stress on Model C under oblique loads of 200 N	30
Figure 14 Maximum Principal Stress on Model D under oblique loads of 200 N	30
Figure 15 Maximum Compressive Stress in all models	32
Figure 16 Maximum Tensile Stress in all models	33
Figure 17 Minimum Principal Stress distribution pattern on Model B under vertical loads of 200 N	34
Figure 18 Maximum Principal Stress distribution pattern on Model B under vertical loads of 200 N	35

Figure 19. Von Mises stress along the cortical bone-implant interface on  
the side of the stress concentration under vertical and oblique loads of 200 N.

## **Chapter I**

### **Introduction**

#### **Background and rationale**

The use of osseointegrated dental implants to restore missing portions of a patient's occlusion has proven to be a successful treatment modality.<sup>1-2</sup> Factors associated with successful osseointegration of a dental implant include implant biocompatibility, implant surface characteristics, implant geometry, implant diameter and implant length.<sup>3</sup> The latter, adequate implant length, has been associated with high implant survival rates and a favorable prognosis.<sup>4-5</sup> However, placement of longer implants is not always feasible due to anatomical limitations, such as the position of the inferior alveolar nerve in the mandibular arch or the possibility of sinus pneumatization in the maxillary arch. With resorbed alveolar ridges, bone augmentation procedures are necessary to regain vertical height in order to accommodate implants of the desired length. Such advanced surgical techniques, including autogenous block grafting or nerve repositioning, are associated with a high level of morbidity.<sup>6</sup> Therefore, in the severely resorbed posterior edentulous areas, placement of short implants offers a simpler alternative for patients. Not only does it avoid potential vital structure injury, it can also shorten overall treatment time.

Recent literature reviews reported comparable survival rates between short implants and standard or long implants.<sup>7-8</sup> This interesting finding has led many implant manufacturers to produce short implants for the benefit of patients and clinicians. Clinical application of these implants involves mainly the posterior maxilla and mandible where there is limited vertical bone height. When restoring these short implants, in order to occlude with the opposing dentition, the implant crown will be moderately longer than the implant fixture within bone. This results in a disproportionate crown-to-implant ratio. As vertical and lateral forces are exerted on these implant crowns, it creates a Class I lever situation. The occlusal loads on implants may create a bending moment, increasing stress concentration on the crest of the alveolar ridge at the implant-to-tissue interface, thus causing potential crestal bone loss.<sup>9</sup>

Multiple methods have been used to study the influence of the biomechanical environment on implant restorations, notably the finite element (FE) method. This method has been used to predict stress distribution patterns in the implant-bone interface in different clinical scenarios.<sup>10</sup> This tool allows for an effective method of investigation of complex systems such as the implant-bone system.

## **Objectives**

1. To evaluate the stress distribution patterns on crestal bone of a short implant ( $\text{\O}5 \text{ mm} \times 6 \text{ mm}$ , plateau-designed, press fit implant) connected to differing crown heights.
2. To compare the stress distribution patterns on crestal bone of a short implant ( $\text{\O}5 \text{ mm} \times 6 \text{ mm}$ ) to those of a regular implant ( $\text{\O}5 \text{ mm} \times 11 \text{ mm}$ ) connected to differing crown heights.

## **Hypothesis**

### **Null Hypothesis (H0)**

There will be no significant difference in stress distribution patterns on crestal bone of a short implant connected to differing crown heights. Also, there will be no significant difference in stress distribution patterns on crestal bone of a short implant compared to those of a regular implant connected to differing crown heights.

### **Alternative Hypothesis (H1)**

There will be a significant difference in stress distribution patterns on crestal bone of a short implant connected to differing crown heights. Also, there will be a significant difference in stress distribution patterns on crestal bone of a short implant compared to those of a regular implant connected to differing crown heights.

**Keywords**

Short dental implants

Survival

Stress distribution

Crown-to-implant ratios

Three-dimensional finite element analysis

**Limitation**

Due to the complexity of three-dimensional implant modeling, short implants produced by only one manufacturer were included in the study. Other short implants available on the market should be included in future studies to compare variations in stress distribution patterns.

**Benefits of study**

This simulation generates visible stress distribution patterns on surrounding bone of implants under loading conditions. It helps a clinician to understand and to visualize the effect on bone after restoring a short implant with a crown having a disproportionate crown-to-implant ratio, otherwise not observable in patients. Moreover, it predicts the stress concentration on crestal bone when these restorations are subjected to various loading conditions.

## Chapter II

### LITERATURE REVIEW

The use and survival of short dental implants

Crown-to-implant ratios

Crestal bone loss and stress distribution

Finite element analysis

#### **The use and survival of short dental implants**

Implant length is the dimension measured from the platform to the apex of an implant.<sup>5</sup> Though no universal definition is available, various authors set their own criteria for short dental implants and most describe it as a designed intra-bony device from 7 mm to 10 mm in length.<sup>7,11</sup> In general, 10 mm or less is considered to be a short dental implant. Historically, it has been recommended to use the longest implant wherever possible.<sup>5</sup> Advantages of increased implant length include increased initial stability, long-term resistance to bending moment forces, expedited healing and decreased risk of movement at the implant-bone interface.<sup>9</sup> For these reasons, short implants were not widely used in clinical practice.

Nowadays, there is a wide variety of application for implants, ranging from single tooth replacement to full mouth reconstruction with a high success rate. In 1981, Adell et

al.'s 15-year study on osseointegrated implant in the treatment of edentulous jaws showed success rates of 81% in the maxilla and 91% in the mandible.<sup>1</sup> However, no data on implant diameter and length was provided. Another longitudinal study on implant survival followed 660 implants for 5-12 years. The authors reported a higher number of implant loss for short Branemark implants placed in the posterior maxilla compared to long implants. Implants of 7mm long had a failure rate of 9.5% compared to 3.8% for all other lengths.<sup>12</sup> As observed by Goodacre et al., the number of implants lost increased with the use of short implants and implant placement in poor bone quality.<sup>13</sup>

Implant length and diameter in relation to implant survival was further studied by Winkler et al.<sup>4</sup> A total of 2917 implants were evaluated and followed for 36 months. Shorter implants had significantly lower survival rates compared to longer implants, with only a 66.7% survival rate for 7mm long implants. The retrospective study by Scurria et al. analyzed a total of 384 implants placed and subsequently restored with 108 prostheses.<sup>14</sup> It was concluded that shorter implants and implants with diameters of less than 4 mm had decreased survival probability.<sup>14</sup> Thus, wherever possible implants were recommended to be as long and as wide as possible within the anatomical limitations of the patient.

More recently, Renouard and Nisand conducted a structured review evaluating the impact of implant length and diameter on survival rates.<sup>7</sup> A total of 53 human studies were included. The authors defined a short implant as one having a length of 8mm or less and a wide diameter implant as one with a width of 4.5mm or more. The highest failure rates for short implants were reported in the older studies, which performed routine surgical procedures without any regard for the bone quality and used machined-surface

implants. The belief was that short implants had reduced bone-to-implant contact; thus, lower survival rates were expected when compared to longer implants. For many years, the prognosis for short implants was unclear. However, more recent studies have reported comparable survival rates for short implants with wide diameters to those obtained with long-implants having standard-diameters. In a retrospective study, Grant et al. studied survival of 335 short dental implants of 8 mm in length.<sup>15</sup> The survival rate for 8-mm long implants placed in the mandible was 99% after 2 years. Advantages of short implants were described as shorter treatment time, lower cost, less discomfort, less surgical risk, and greater surgical ease. Therefore, short-length (8 mm) dental implants would offer an effective treatment alternative to bone grafting and nerve repositioning for the atrophic posterior mandible.

The latest review by Romeo et al. analyzed the literature published from 2000 to 2008 comparing short implants (10 mm or less) to standard/long ones.<sup>16</sup> A total of 13 articles were included in this review. Most of the studies reported different survival rates for short and standard implants, though the difference was insignificant. In the same year, a retrospective cohort study evaluated the survival rates of short dental implants in the posterior jaws. These implants were followed for 1-8 years.<sup>17</sup> Six hundred and sixty one patients received 1287 short Biotechnology Institute (BTI) implants ( $\leq 8.5$  mm) from 2001 to 2008. This study showed an implant-based survival rate of short implants of 99.3% with 1-8 years of follow up. The authors suggested that the use of short implants following strict clinical protocols could achieve predictable outcomes. Most of the current publications show similar survival rates for short and standard implants. These

authors emphasize that treatment planning is a key factor for the success of short implants.

Rough implant surfaces have also been evaluated for their effect on implant survival. Kotsovilis et al. conducted a systematic review and meta-analysis on the effect of implant length on the survival of rough-surface dental implants.<sup>8</sup> Thirty-seven articles met the inclusion criteria. The meta-analysis revealed no statistically significant difference in the survival between short ( $\leq 8$  or  $<10$  mm) and conventional ( $\geq 10$  mm) rough-surface implants placed in totally or partially edentulous patients. When the placement of conventional implants was impossible or when extensive advanced surgical procedures was required, it was recommended that clinicians use short implants as an efficacious treatment modality for the replacement of missing teeth in totally and partially edentulous patients.

### **Crown-implant ratios (C/I)**

The crown-to-implant (C/I) ratio is the relationship between the length of the crown and the length of the implant embedded in bone. Implant length is the measurement from the apex to the most coronal bone-implant contact, while crown length is the distance from the occlusal surface of the crown to the most coronal bone-implant contact. A favorable C/I ratio guideline has not been established in the dental literature unlike crown-to-root ratios for natural teeth, which has been helpful for clinicians in determining prognosis of treated teeth.

In general, it is assumed that the use of short implants with limited alveolar bone height due to resorption leads to a greater C/I ratio. Under occlusal forces, the implant crown acts as a lever arm. This creates a bending moment and transfers the stress to the peri-implant crestal bone which may cause bone resorption.<sup>18</sup> Crestal bone remodeling is an initial predicting factor for implant failure. As the crestal bone resorption progresses, the crown height increases. The stress in the cancellous bone also increases and implants subjected to lateral load may result in implant failure.<sup>18</sup>

Lately, interesting new findings have been reported regarding the effect of C/I ratio on surrounding bone. Blanes et al. conducted a longitudinal prospective study on the influence of C/I ratio on crestal bone loss around dental implants placed in the posterior region.<sup>19</sup> The results showed the mean clinical C/I ratio was 1.77. Cumulative survival rates for the group with a C/I ratio equal to or greater than 2 was 94.1%. Contrary to general belief, higher C/I ratio was associated with less crestal bone loss.

A systematic review of 2 selected randomized-controlled clinical trials with at least a 4 year follow-up period showed that C/I ratio of implant-supported restorations did not influence the peri-implant crestal bone loss.<sup>20</sup> Schulte et al. was the first to evaluate the C/I ratio on single tooth implant-supported restorations and to compare it to the guideline established for crown-to-root ratio of natural teeth.<sup>21</sup> A total of 889 single tooth implants were included in the study. The survival rate was 98.2 % with a mean follow-up time of 2.3 years and the mean C/I ratio of implants in function was 1.3. It was suggested that the guideline used for natural teeth should not be applied to potential implant sites or existing implant-supported restorations. In 2010, a radiographic retrospective cohort study by Birdi et al. investigated the C/I ratio of single implant-

supported restorations on short-length plateau-design implants.<sup>22</sup> In this study, three hundred and nine plateau-design implants with either 5.7 mm or 6 mm in length were investigated. Mean follow-up time was 20.9 months. Mean C/I ratio was 2.0. The average mesial and distal first bone-to-implant contact levels were 0.2 and 0.2 mm, respectively. There was no association between C/I ratio and first bone-to-implant contact levels. It was concluded that C/I ratio did not affect the success of the short-length plateau-design implants.

### **Crestal bone loss and stress distribution**

The majority of clinical complications of osseointegrated implants are related to biomechanical factors, such as types of prosthesis and implant length.<sup>13</sup> The close apposition of bone to the titanium implant is the essential feature that allows for transmission of stress from the implant to the bone without any appreciable relative motion or abrasion.<sup>23</sup>

A key factor for the success or failure of a dental implant is the manner in which stress is transferred to the surrounding bone.<sup>24</sup> Factors influencing load distribution on implants include gender, age, location of implant in the arch, and parafunctional habits.<sup>25</sup> When the implants are subjected to unfavorable occlusal forces, stress accumulates in the crestal region and crestal bone remodeling is observed. Crestal bone loss has been observed around the perimucosal area of dental implants for decades. Crestal bone stability is one of the criteria used to evaluate the success of dental implants.<sup>26,27</sup> Adell et al. were the first to quantify the amount of crestal bone loss in a 15-year study on osseointegrated implants on edentulous jaws.<sup>1</sup> Marginal bone loss was measured at the

time the abutment was connected, then 6 and 12 months postoperatively. These non-loaded implants already exhibited a mean bone loss of 1.5 mm during the healing period and the first year after abutment connection. Thereafter, only 0.1 mm of marginal bone was lost annually in the group observed for 5-9 years. Branemark et al. also reported a 1 to 1.5 mm crestal bone loss during the first year after abutment connection.<sup>27</sup> This crestal bone loss was attributed to surgical trauma at the time of implant placement. After the initial crestal bone loss, only 0.1 mm bone loss per year would be expected.

### **Finite element analysis**

The finite element method (FEM) is a numerical method of analysis for stresses and deformations in structures of any given geometry. The structure is discretized into the so-called “finite elements” which are connected through nodes. This method has become one of the most successful engineering computational methods and the most useful analytical tool for decades.

Finite element analysis (FEA) has been extensively used to predict biomechanical performance of dental implant.<sup>10</sup> It allows researchers to investigate stress distribution at the implant-bone interface within cortical and trabecular bone. Implant geometry causing unfavorable stress distribution patterns may contribute to pathologic bone resorption or bone atrophy.<sup>24</sup> Due to the complexity of the implant-bone system, FEA was considered to be the most suitable tool for analysis.

Load transfer at the implant-bone interface depends on the type of loading, material properties of the implant, implant geometry, implant length and implant

diameter.<sup>24</sup> Also, specific morphological characteristics of various commercial dental implants affects clinical performance. Among these factors, FEA has been applied extensively to study different components of implant geometry, namely the implant-abutment connection, the crest module of an implant, and the implant length.

There is a large amount of literature available on implant-abutment connections. Chun et al. studied the type of implant abutment and its influence on stress distribution in bone under various loading conditions using FEA.<sup>29</sup> The authors concluded that implant-abutment connection affected stress distribution in bone, with the internal-hex implant system generating the lowest Von Mises stress possible under all loading conditions evaluated. Meanwhile, Kitagawa et al. used a nonlinear transient dynamic analysis under impulsive loadings to compare internal-hex, taper connection implants (Ankylos) and external-hex implant connection.<sup>30</sup> Findings revealed greater movement associated with the external-hex connection as compared to the tapered connection. In addition, differences were observed in the rotation of components between dental implant systems using a taper or an external-hex connection. A subsequent FEA study by Quaresma et al. showed that internal-hex connection produced higher stresses on the alveolar bone compared to the conical connection.<sup>31</sup> Based on the results from using a simulated 3D model of an external-hex implant connected to different abutment size, Maeda et al. suggested the use of a smaller diameter abutment with a larger implant diameter (platform-switching configuration). This configuration offered various biomechanical advantages as it shifted the stress concentration area away from the crestal bone.<sup>32</sup> Tabata et al. presented similar results with a platform-switched implant using 2D FEA. Superior biomechanical behavior was noted in terms of the stress distribution in the implant

fixture. This implant design had better stress distribution on the bone, showing a reduction in the maximum stress by 80%.<sup>33</sup> However, there was higher stress concentration in the crown and retention screw.

Furthermore, studies have been conducted focusing on the relation between the crest module of an implant and the stress in the bone. Shi et al. described the optimized dental implant design that reduced crestal bone stress. In this 3D optimized design, the important features required to reduce the peak stress at the crestal bone are a tapered crest module and wider implant diameter.<sup>34</sup> These findings are supported by Bozkaya et al. That study evaluated how the external contour of an implant contributed to various bone failure modes.<sup>35</sup> Through 2D FEA, the crest module of implant with narrowing cross-sections at the top of the cortical bone created more favorable load transfer characteristics in single-tooth implants. Thus, this body and thread design for a dental implant were advocated to minimize stress distribution on bone.<sup>36-37</sup>

Implant length is another topic of interest that has been analyzed by many studies, most of which used FEA. The optimal length of a dental implant is difficult to define but past studies have shown that implant length is more important than implant diameter at reducing bone stress and achieving implant stability. Li et al. used this method to define the optimal implant diameters and length in posterior maxillary type IV bone.<sup>38</sup> Included in the study were implant diameters ranging from 3.0 to 5.0 mm, and implant lengths ranging from 6.0 to 14 mm. It was suggested that implants wider than 4 mm and longer than 9 mm were the optimal selection for implants planned in type IV bone. Around immediately loaded implants, Ding et al. showed that increasing implant diameter and length resulted in lessened stress and strain on the crestal bone.<sup>39</sup> However, implant

diameter had a more significant effect than length to relieve the crestal stress and strain concentration. This study exerted vertical and oblique loading of 150 N on seven implant designs, which resulted in combinations of implant diameters ranging from 3.3 to 4.8 mm and lengths ranging from 6 to 14 mm.

Subsequently, Baggi et al. studied the influence of implant diameter and length on stress distribution of 5 different implant designs.<sup>40</sup> Numerical results also suggested that implant diameter might be more effective than implant length at minimizing stress distribution around the bone. In addition to implant length and diameter, Anitua et al. also examined the influence of implant geometry on stress distribution.<sup>17</sup> A force of 150 N was applied at an angle of 30 degrees. The four-implant systems studied (Tiny, Interna Universal, Interna Plus, and Interna Wide) showed there was a significantly greater effect of implant diameter on stress distribution in bone than implant length or geometry. Maximum stress was located around the neck of the implant and distributed in the bone adjacent to the first six threads of the implant. This could possibly imply that use of short and wide implants may be a reasonable alternative in limited bone scenarios.

In addition to implant length and diameter, another study evaluated the influence of implant taper on strains in the crestal bone using 3D FEA.<sup>41</sup> Petrie and Williams used various implants with a diameter ranging from 3.5 to 6 mm, length ranging from 5.75 to 23.5 mm and a taper form ranging from 0 to 14 degrees: this allowed for a total of 16 implant designs. These implants were subjected to oblique occlusal loading (200 N vertical and 40 N horizontal). While evaluating the maximum shear strain in the crestal bone, the authors found that increasing implant length and diameter reduced strain on

bone. Hence, the use of a wide and relatively long untapered implant seems to be the most favorable choice.

Resorption patterns around implants caused by stress on crestal bone were analyzed by Kitamura et al.<sup>18</sup> The authors evaluated both pure vertical resorption and conical resorption. With the pure vertical resorption models, as the bone resorption progressed, implant crown height automatically increased. The stresses of the cortical and cancellous bone increased with resorption depth.

Recently, the use of short implant for patients has increased due to the reported increased survival rates. More than 220 implant brands have been identified, produced by about 80 manufacturers. Implants are manufactured and sold without providing any clear evidence to the claims of alleged benefits of specific morphological characteristics of dental implants.<sup>42</sup> One such implant system (Bicon; Bicon Inc, Boston, Mass) incorporates the taper shoulder, locking taper connection, and smaller abutment diameter. Although this system offers short implants to the market, there has been no investigation using the FE method to analyze the effect of such short and wide dental implants connected to differing crown heights. Therefore, the purpose of this study is to evaluate the stress distribution patterns on crestal bone of a short implant ( $\varnothing 5$  mm $\times$ 6 mm, plateau-designed, press fit implant) connected to differing crown heights. Additionally, this study will evaluate the stress distribution patterns on crestal bone for a short implant ( $\varnothing 5$  mm $\times$ 6 mm.) and compare those findings to regular implants ( $\varnothing 5$  mm $\times$ 11 mm.) connected to similar crown heights.

## Chapter III

### Material and methods

#### Material

**Dental implant** (Bicon; Bicon Inc, Boston, Mass)  $\varnothing 5$  mm $\times$ 6 mm Integra-CP<sup>TM</sup> Part Number 260-350-306

**Dental implant** (Bicon; Bicon Inc, Boston, Mass)  $\varnothing 5$  mm $\times$ 11 mm Integra-CP<sup>TM</sup> Part Number 260-350-311

**Abutment**  $\varnothing 5$  mm $\times$ 5 and  $\varnothing 5$  mm $\times$ 9 mm, zero degree, 3 mm post, Part Number 260-350-050

**A micro-CT scanner** (X-TEK XT H 225;Metris, Leuven, Belgium)

#### Methods

##### Software used

**Altair Hypermesh** (Hyperworks; Altair Engineering, Inc, Troy, Mich)

**Amira** (Amira;Visage Imaging GmbH, Berlin, Germany)

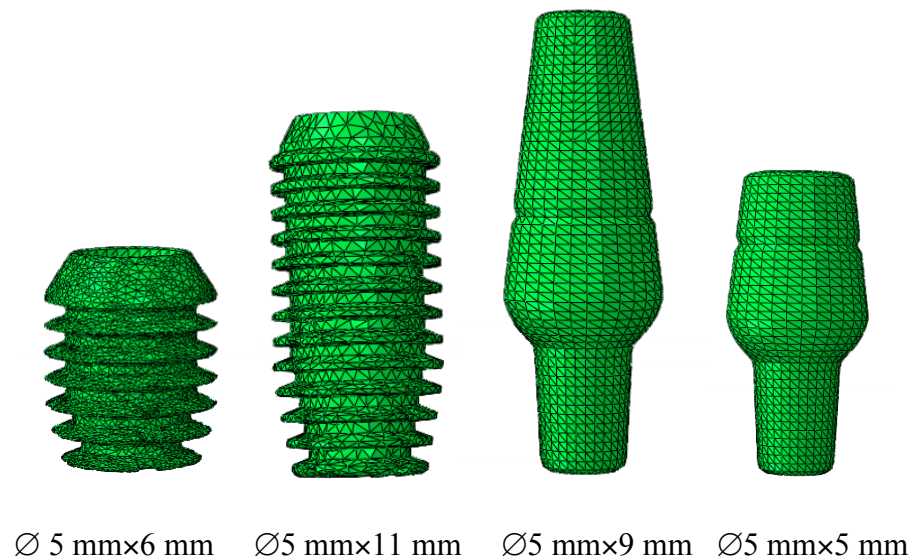
**VG Studio Max 2.0** (VG Studio Max 2.0; Volume graphics GmbH, Heidelberg, German)

**CTpro** (Metris; Leuven, Belgium)

**Abaqus CAE**, (ABAQUS CAE; Hibbitt, Karlsson & Sorensen, Inc, Plymouth, Mich)

Two implant designs were selected for the three-dimensional finite element modeling. Bicon implants of  $\text{Ø}5 \text{ mm} \times 6 \text{ mm}$  and  $\text{Ø}5 \text{ mm} \times 11 \text{ mm}$ , abutments of  $\text{Ø}5 \text{ mm} \times 9 \text{ mm}$ , and abutment  $\text{Ø}5 \text{ mm} \times 5 \text{ mm}$ , zero degree, 3 mm post (Bicon; Bicon Inc, Boston, Mass) were scanned using a high resolution micro-CT scanner (X-TEK XT H 225;Metris, Leuven, Belgium) to obtain accurate geometry of the implants and abutments (Figure 1).

Figure 1. Implant and Abutment Geometry



The images of implants and abutments were reconstructed by software CT pro 2.0 (Metris; Leuven, Belgium). STL surface models were then extracted using VG Studio

Max 2.0 (VG Studio Max 2.0; Volume graphics GmbH, Heidelberg, German). The STL files were imported to Amira (Amira; Visage Imaging GmbH, Berlin, Germany) in order to generate surfaces of implants and abutments. Mesh refinement and modeling were performed using Hypermesh (Hyperworks; Altair Engineering, Inc, Troy, Mich). The abutment was connected to each implant. The abutment and implant body were adopted as a single unit. This eliminated any potential influence from the micro-movement between components. The surrounding bone was modeled as a cylinder with a 14 mm diameter and 17 mm height around each implant as shown in Figure 2.

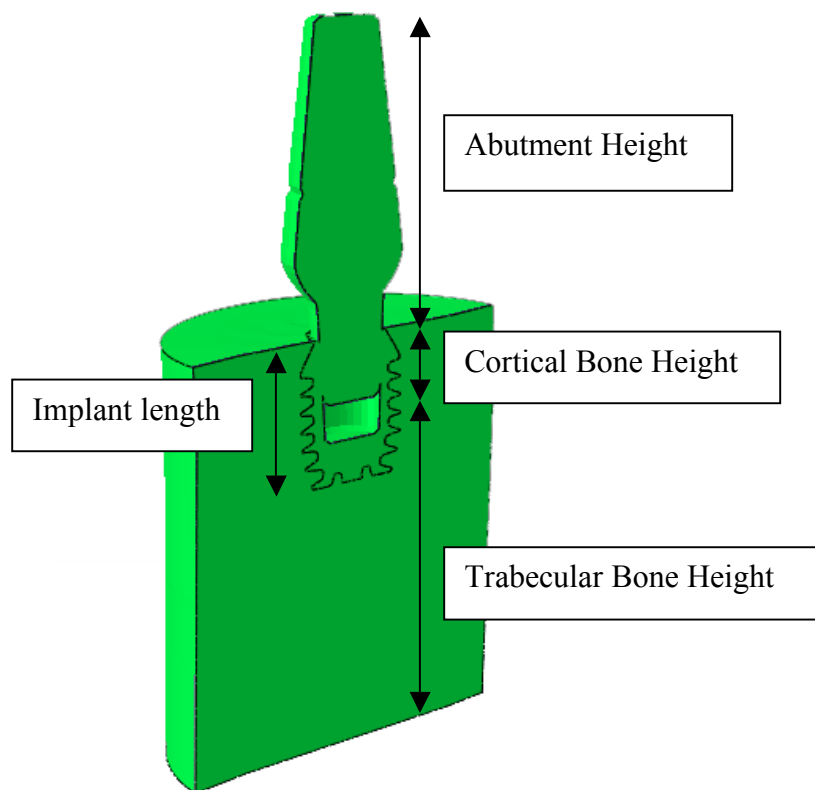


Figure 2. Key measurements of model

The bone model was sufficiently large compared to the implant dimensions such that the boundary conditions were irrelevant over the area analyzed for stress distribution. Gingival soft tissues were not modeled as they were much softer than the other components. Cortical bone and trabecular bone were assumed to be homogenous, isotropic, and linearly elastic and the material properties used in the 3D FE model are shown in Table 1. These properties represent type II bone quality.<sup>43</sup> This bone has a thick cortical layer surrounded by dense trabecular bone of favorable strength.

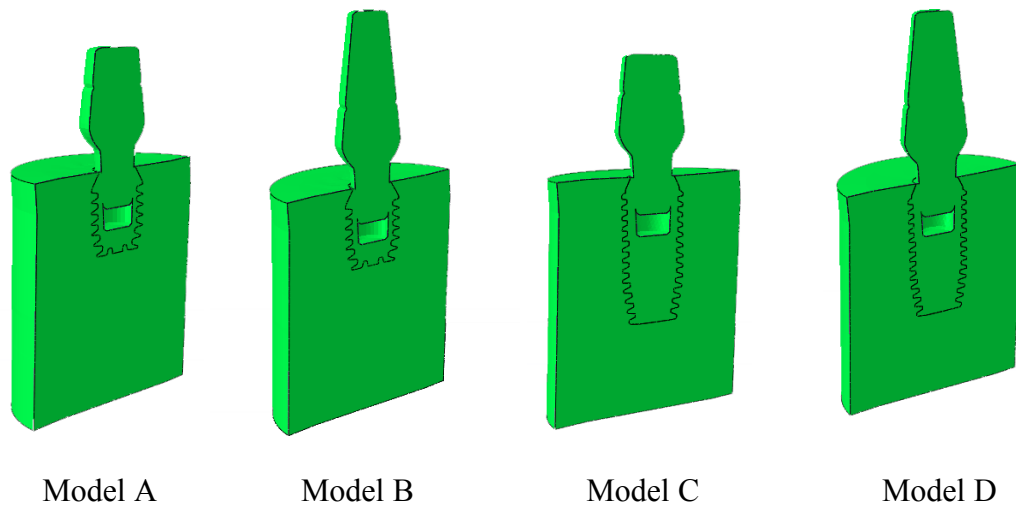
Table 1. Young's Modulus and Poisson's Ratio of Materials Used.

Materials	Young's Modulus (GPa)	Poisson's ratio
Abutment(Ti6Al4V) <sup>29,35-36,41</sup>	114	0.34
Implant (Ti6Al4V) <sup>29,35-36,41</sup>	114	0.34
Cortical bone <sup>44,35-36</sup>	14.0	0.32
Trabecular bone <sup>34,46</sup>	1.37	0.40

Cortical bone and trabecular bone were separated. Cortical bone was modeled to the same level as the implant platform. The thickness of cortical bone was assumed to be 2 mm.<sup>29</sup> Tetrahedral iso-parametric elements were used for the mesh. The external surfaces of the bone model were constrained on the vertical walls and the inferior wall of the bone models. Nonlinear contact with a frictional coefficients of 0.2 was assumed between the abutment and implant in the locking taper connection. Implants were considered to be perfectly osseointegrated.

Stress analysis was performed for four models: Model A, a short implant ( $\varnothing 5$  mm $\times$ 6 mm) connected with a regular abutment ( $\varnothing 5$  mm $\times$ 5 mm); Model B, a short implant ( $\varnothing 5$  mm $\times$ 6 mm) connected with a long abutment ( $\varnothing 5$  mm $\times$ 9 mm); Model C, a regular implant ( $\varnothing 5$  mm $\times$ 11 mm) connected with a regular abutment ( $\varnothing 5$  mm $\times$ 5 mm) as a control model; and Model D, a regular implant ( $\varnothing 5$  mm $\times$ 11 mm) connected with a long abutment ( $\varnothing 5$  mm $\times$ 9 mm) (Figure 3). This resulted in a C/I ratio of 1.33/1, 2/1, 0.7/1, 1.09/1 for Model A, B, C, and D respectively. (Figure 3)

Figure 3. Implant-bone models



The number of elements and nodes contained in the models are given in Table 2.

Table 2. Number of elements and nodes used in the FE models

Components	Number of Elements	Number of Nodes
Bicon implant (5×11 mm)	42225	11732
Bicon implant (5×6 mm)	26656	7638
Long abutment	11972	2944
Abutment	8165	2097
Cortical bone	38687	9073
Cancellous bone	107604	24178

All models were imported to Abaqus CAE, (ABAQUS CAE; Hibbitt, Karlsson & Sorensen, Inc, Plymouth, Mich) for analysis. Two loading conditions were simulated on each implant model: pure vertical and oblique loads. An oblique load was simulated by applying a 100 N load at a 15-degree angle from the vertical axis to the central node on the occlusal surface of the abutment. This consisted of a 96.3 N vertical component and a 26.8 N lateral component.<sup>44,45</sup> Also, additional loading conditions included the application of a 200-N and a 700-N (overload condition) oblique force. The 100, 200, and 700 N (overload condition) pure vertical loading conditions were also tested. The 700 N was assumed to be forces generated by bruxers which are as much as four to six times higher than those of non-bruxers.<sup>47</sup> Since bone can be classified as a brittle material, the principal stresses were used to evaluate the stress distribution pattern around the crestal region. The highest maximum and minimum principal stresses exerted on the bone of each model were used for comparison. Stress distribution patterns along each implant

were analyzed and compared among the 4 models.

Bone failure can be defined as local fracture of the bone due to excessive local loads. Assuming that ultimate bone strength is the physiological limit, local overloading at cortical bone occurs during compression, at a maximum compressive principal stress exceeding 170-190 MPa in modulus, and under tension, at a maximum tensile principal stress exceeding 100-130 MPa.<sup>41</sup> Similarly, in trabecular bone, local overloading occurs when the most tensile principal stress and/or the most compressive principal stress exceeds 5 MPa.<sup>41</sup>

## Results

With a 100 N oblique load, the peak compressive stress in the models, ranged from 18.30 MPa (Model C) to 27.20 MPa (Model B) (Figure 4). At 200 N, the peak compressive stress in the models, ranged from 36.0 MPa (Model C) to 53.57 MPa (Model B) (Figure 5,6,7,8). At 700 N (overload condition), the peak compressive stress in model A, C, and D, ranged from 127.8 MPa (Model C) to 163.5 MPa (Model D). However, the compressive stress of 193.4 MPa found in Model B exceeded the physiological limit of cortical bone. As crown height increased at 700 N, the peak compressive stress increased by 28.6% (models A and B). For long abutments at 700 N, increasing implant length reduced the peak compressive stress by 15.5% (models B and D) (Table 3).

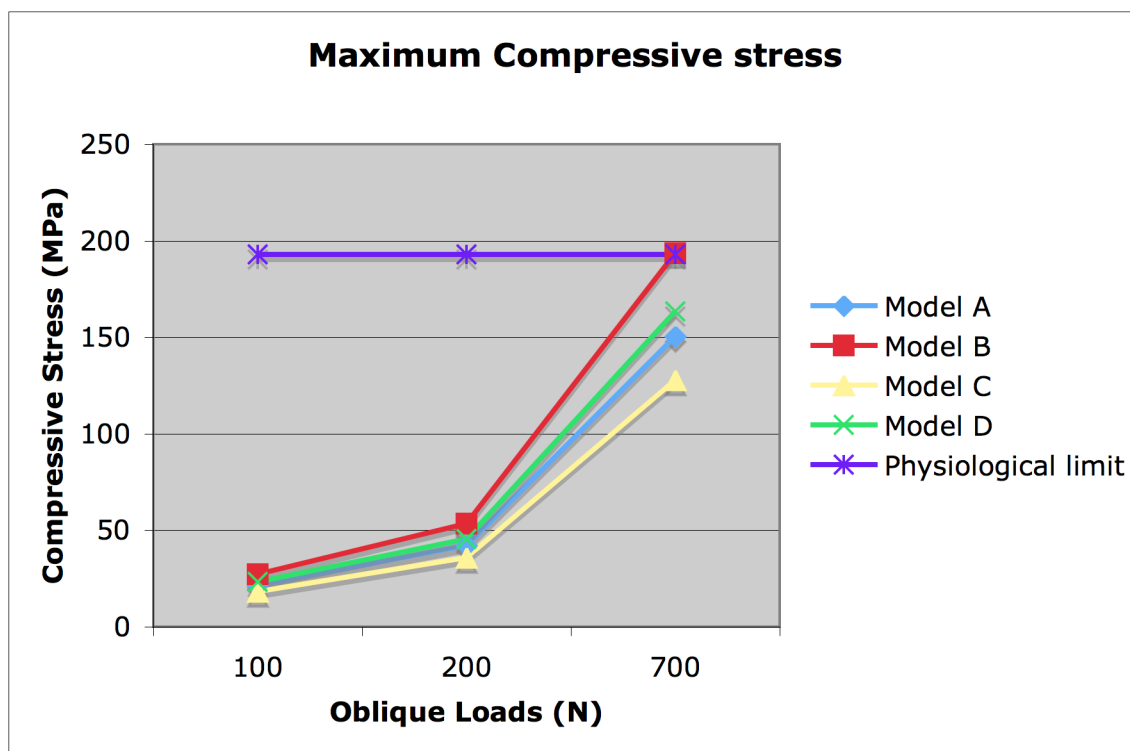


Figure 4. Maximum Compressive Stress of all models

Abutment Height \ Implant length	Implant length	
	6 mm	11 mm
5 mm	150.4 MPa	127.8 MPa
9 mm	193.4 MPa	163.5 MPa

Table 3. Maximum Compressive Stress of all models under oblique loads of 700 N

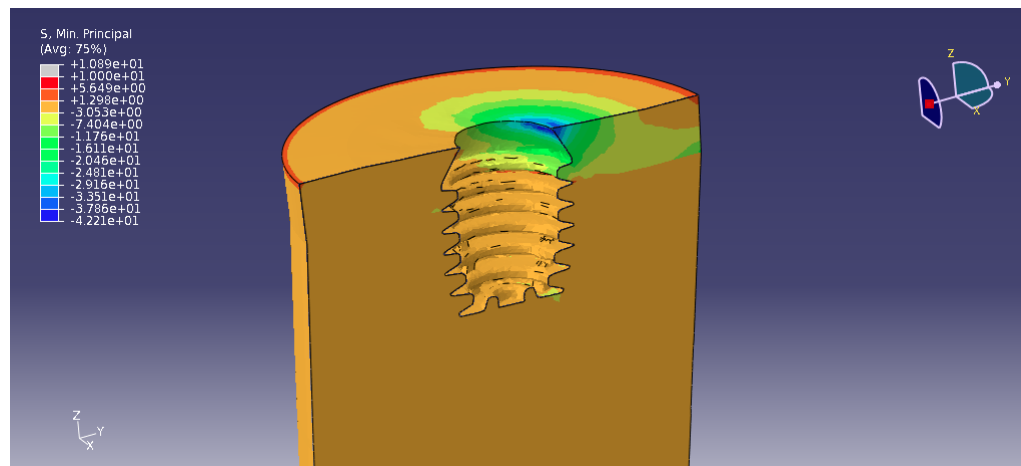


Figure 5. Minimum principal stress on Model A under oblique loads of 200 N

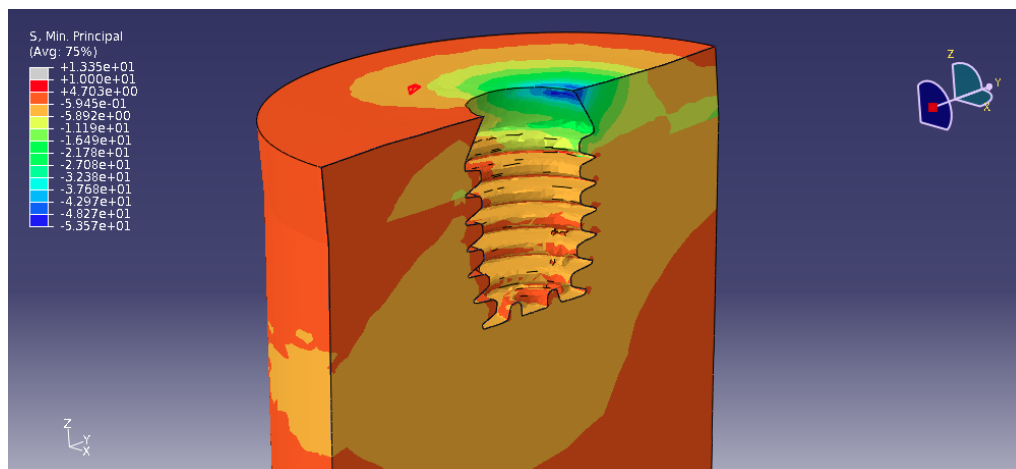


Figure 6. Minimum principal stress on Model B under oblique loads of 200 N

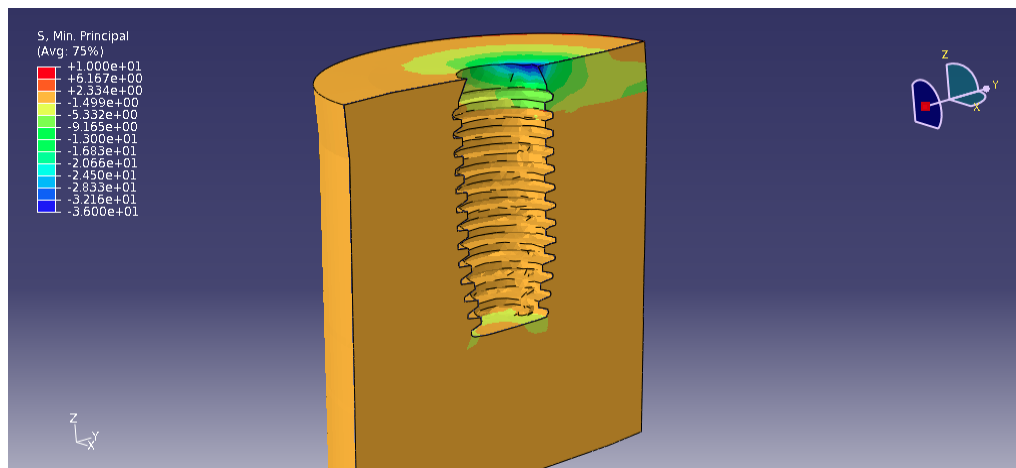


Figure 7. Minimum principal stress on Model C under oblique loads of 200 N

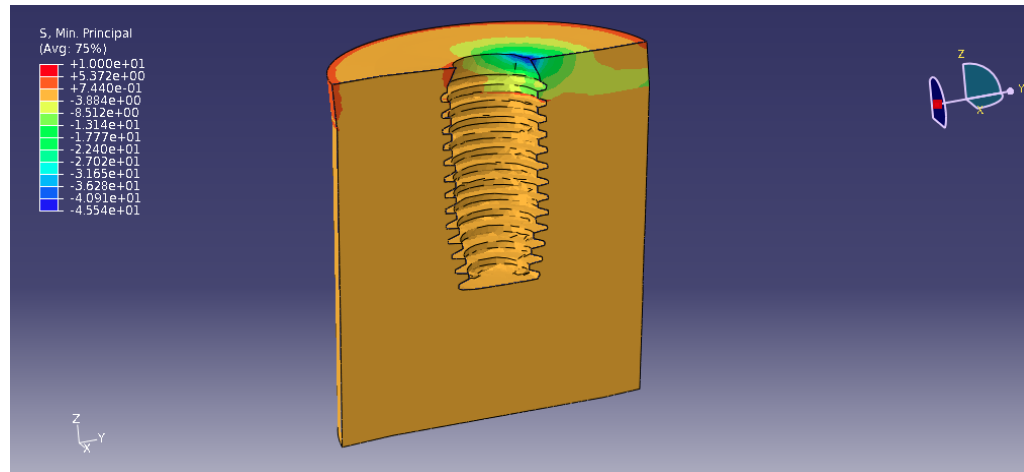


Figure 8. Minimum principal stress on Model D under oblique loads of 200 N

The compressive stress distribution patterns for the oblique loads were relatively similar in all models. A compressive stress concentration was observed on the cortical bone at the area of implant crest module. The area in blue showed the peak compressive stress (Figure 9) and the lesser compressive stresses located at the apex area are shown in light green (Figure 7).

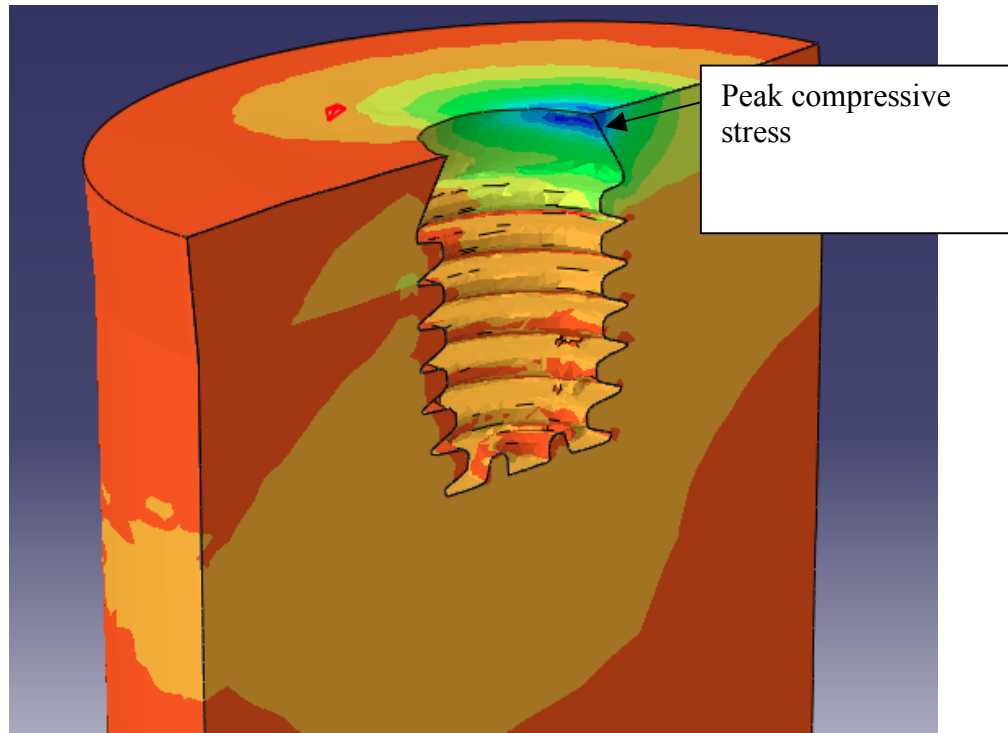


Figure 9. Minimum principal stress distribution pattern in Model B under oblique loads of 200 N

The peak tensile stresses with a 100 N oblique load ranged from 7.39 MPa (Model C) to 22.26 MPa (Model B) (Figure 10). At 200 N, the peak tensile stresses ranged from 14.19 MPa (Model C) to 43.95 MPa (Model B) (Figure 11,12,13, and 14). At 700 N (overload condition), the peak tensile stresses were largest for Model A and B, which were 123.5 MPa and 158.6 MPa respectively. The peak tensile stress in Model B exceeded the physiological limit of cortical bone. At 700 N oblique load, increasing the crown height increased the peak tensile stress by 28.4 % (model A and B). Increasing the implant length reduced the peak tensile stress by 47.6 % (model B and D) (Table 4).

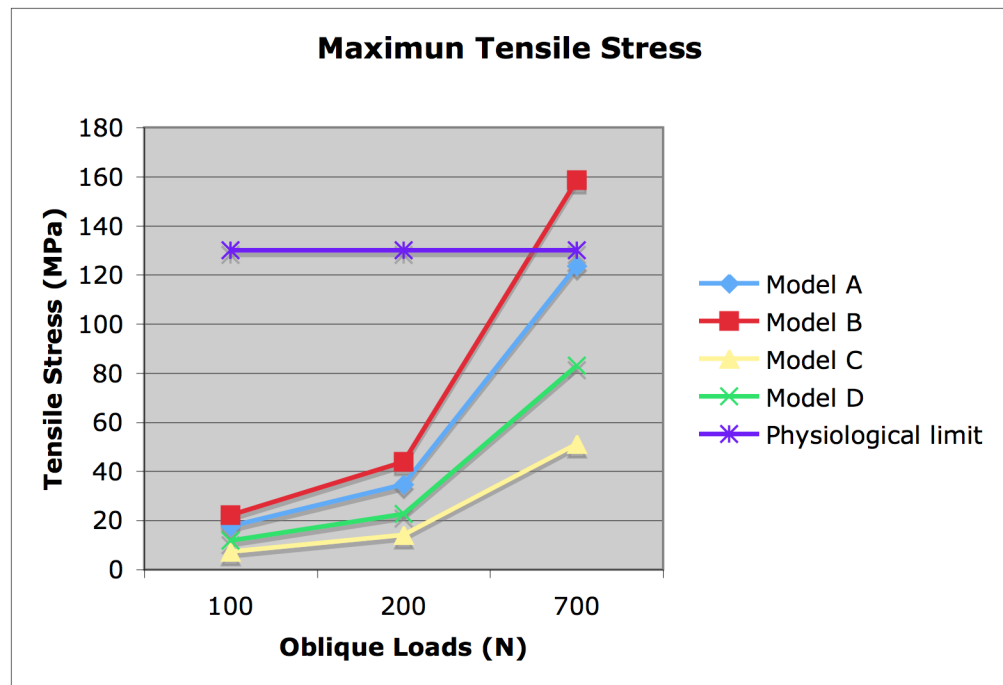


Figure 10. Maximum Tensile Stress of all models

Abutment Height \ Implant length	6 mm	11 mm
	5 mm	123.5 MPa
9 mm	158.6 MPa	83.0 MPa

Table 4. Maximum Tensile Stress of all models under oblique loads of 700 N

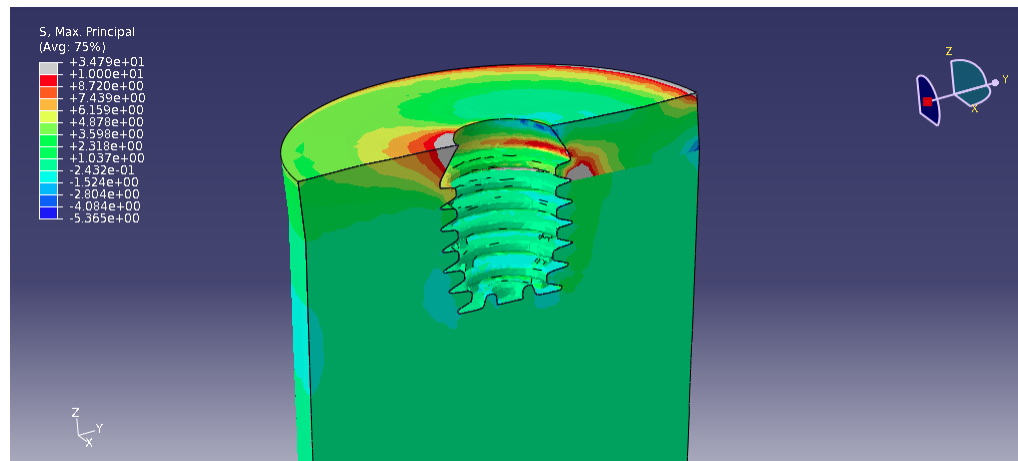


Figure 11. Maximum principal stress on Model A under oblique loads of 200 N

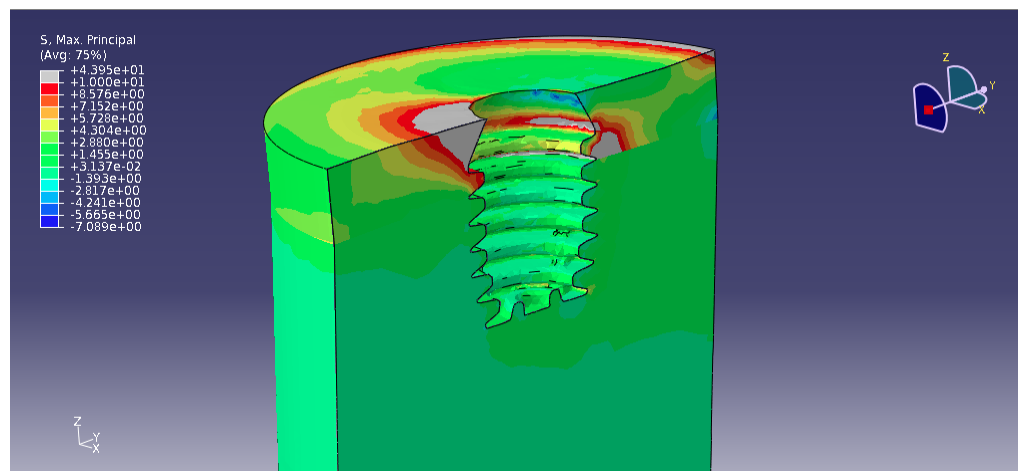


Figure 12. Maximum principal stress on Model B under oblique loads of 200 N

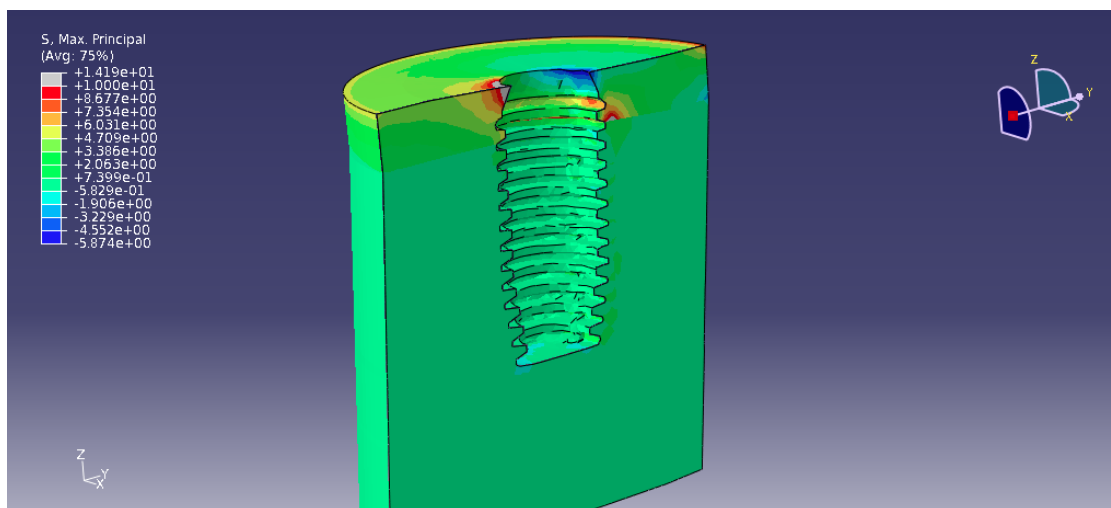


Figure 13. Maximum principal stress on Model C under oblique loads of 200 N

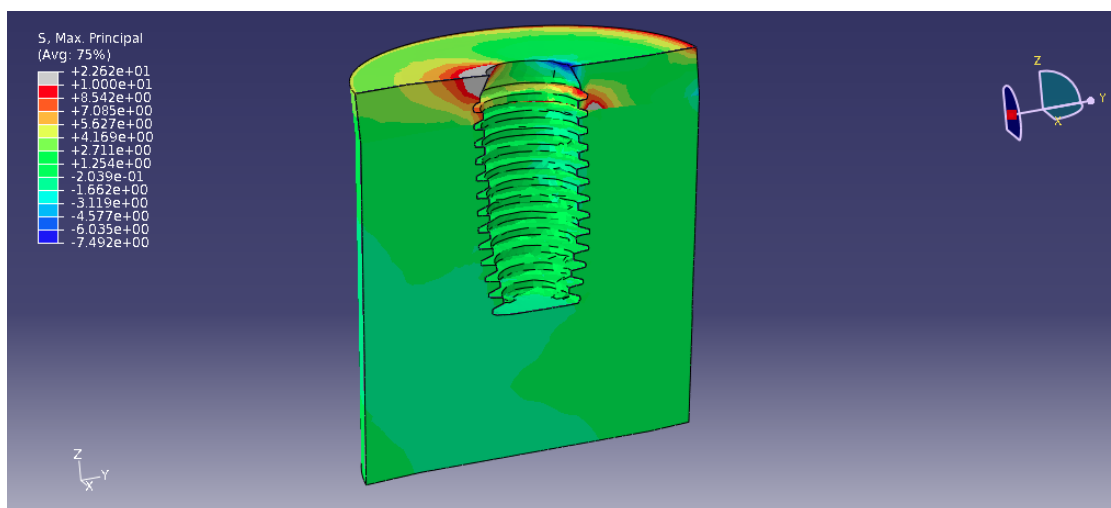


Figure 14. Maximum principal stress on Model D under oblique loads of 200 N

The tensile stress distribution patterns for the oblique loads were relatively similar in all models. A tensile stress concentration was observed in the cortical bone at the area of the implant crest module on the same side as the point of loading (in grey color) (Figure 11,12,13, and14). Tensile stresses also accumulated at the junction between the cortical bone and trabecular bone opposite to the point of loading.

For pure vertical loads, all models showed comparable peak compressive stresses regardless of implant length and crown height (Figure 15). At 700 N (overload condition), the peak compressive stress ranged from 54.0 to 70.87 MPa (Table 5); while peak tensile stresses were highest in Model A and B, at 73.72 MPa and 77.98 MPa, respectively (Table 6). Under overload conditions, lower peak tensile stresses were observed in Model C with 35.76 MPa, and in model D with 36.43 MPa. (Figure 16) Increasing the crown height increased the peak tensile stress by 5.7 % (model A and B). For long abutments (model B and D), increasing implant length reduced the peak tensile stress by 53.28 % (Table 6).

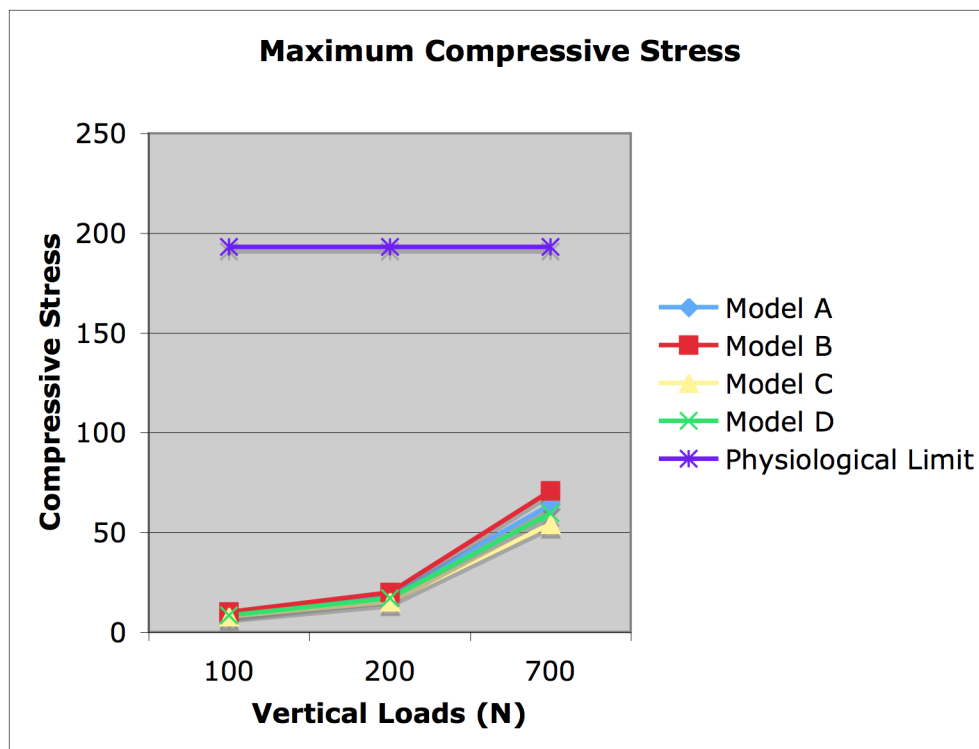


Figure15. Maximum Compressive Stress in all models.

Abutment Height \ Implant length	6 mm	11 mm
	5 mm	63.97 MPa
9 mm	70.87 MPa	59.62 MPa

Table 5. Maximum Compressive Stress of all models under vertical loads of 700 N

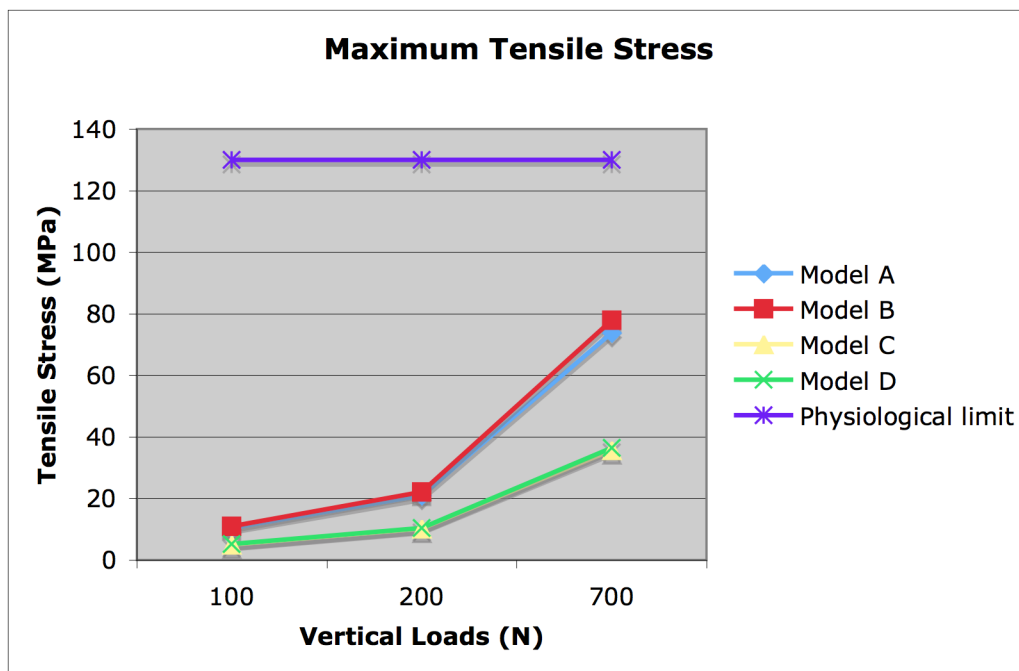


Figure 16. Maximum Tensile Stress in all models.

Abutment Height \ Implant length	Implant length	
	6 mm	11 mm
5 mm	73.72 MPa	35.76 MPa
9 mm	77.98 MPa	36.43 MPa

Table 6. Maximum Tensile Stress of all models under vertical loads of 700 N

The stress distribution patterns for the pure vertical load were relatively similar in all models (Figure 17 and 18). The patterns were symmetric. A compressive stress concentration was observed in the cortical bone at the area of the implant crest module and apex of the implants. Tensile stresses accumulated at the junction between the cortical and trabecular bone, corresponding to the second thread of the implant.

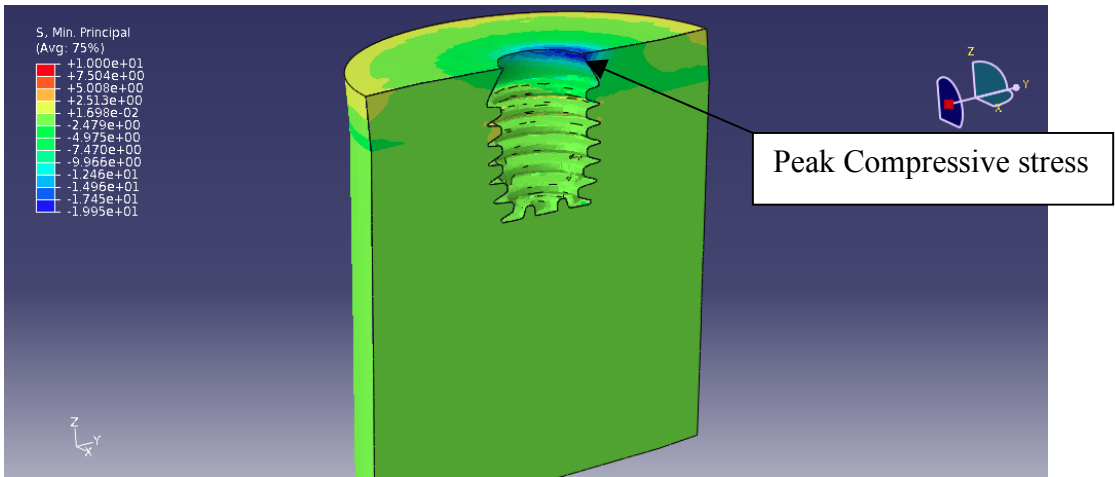


Figure 17. Minimum principal stress distribution pattern on model B under vertical loads of 200 N

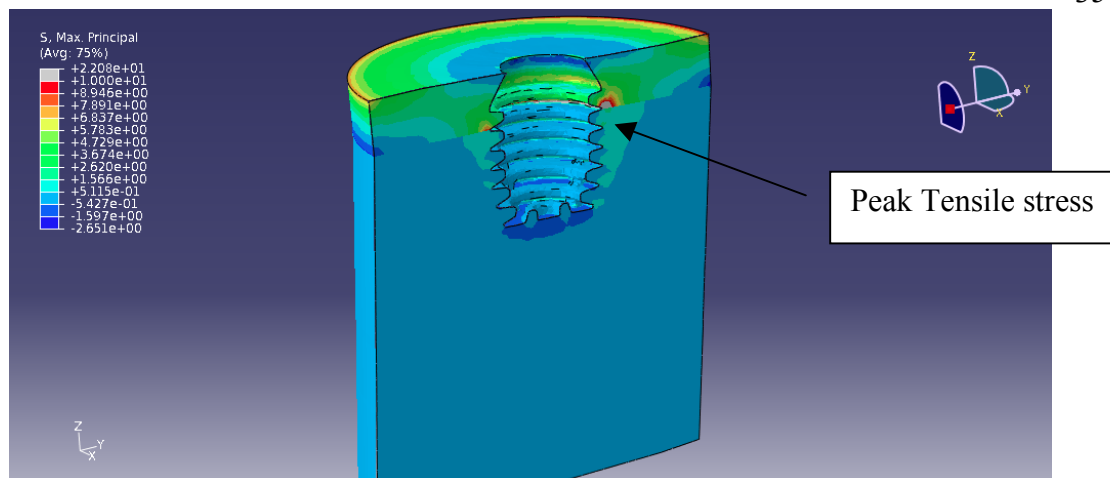
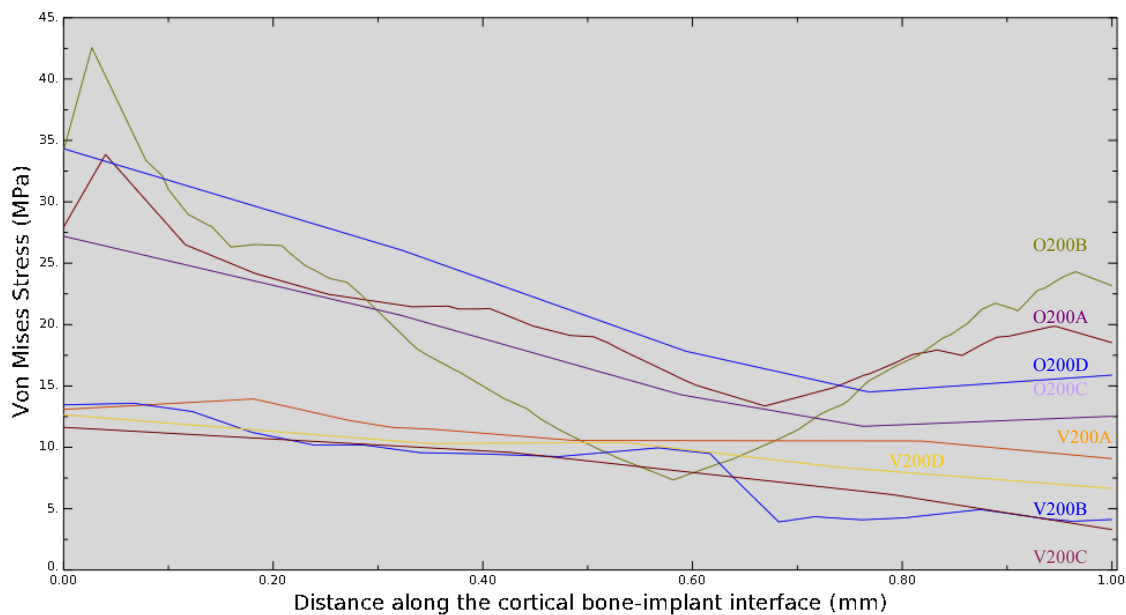


Figure 18. Maximum principal stress distribution pattern on model B under vertical loads of 200 N

The results for all 4 models under vertical and oblique loads of 200 N were compared in Figure 19. Von Mises stresses were used to demonstrate stress concentration on the implant crest module along the implant-bone interface. The patterns of stresses are similar with the peak stresses being at the implant crest module and continuously reducing along the sloping shoulder.



O200A = Model A under an oblique load of 200 N

O200B = Model B under an oblique load of 200 N

O200C = Model C under an oblique load of 200 N

O200D = Model D under an oblique load of 200 N

V200A = Model A under a vertical load of 200 N

V200B = Model B under a vertical load of 200 N

V200C = Model C under a vertical load of 200 N

V200D = Model D under a vertical load of 200 N

Figure 19. Von Mises stress along the cortical bone-implant interface on the side of the stress concentration under vertical and oblique loads of 200 N.

## Discussion

The purpose of this study was to use three-dimensional FE models to evaluate the stress distribution patterns on crestal bone of short implants connected to different crown heights, and to compare these results to those obtained on regular implants. In order to simplify the study, no restorations were placed on the abutments for ease of manipulation, cost-effectiveness and simplicity. Since these simplifying measures were applied to all models, assumptions from one model can be directly compared to the other without affecting the final conclusions.

The data rejects the null hypothesis as there was a significant difference in stress distribution patterns on crestal bone of a short implant connected to different crown heights. Also, there was a significant difference in stress distribution patterns on crestal bone of a short implant compared to those of a regular implant connected to different crown heights

For a given implant geometry, the results of this study showed that the compressive and tensile stress distribution patterns on a Bicon implants were concentrated in the cortical bone at the area of the implant crest module and at the apex of the implant. The observed patterns were in agreement with the shape optimized implant design proposed by Shi et al that was similar to the Bicon design.<sup>34</sup> The authors used a 3D optimized dental implant design to show the important features necessary to reduce the peak stress at crestal bone: a tapered crest module and a wider diameter of implant.<sup>34</sup> Similar results were reported by Bozkaya et al., in a 2D FEA study evaluating the effects of implant external contour on bone failure modes.<sup>35</sup> The crest module of an

implant with narrowing cross-sections at the top of the cortical bone created more favorable load transfer characteristics for single-tooth implants.<sup>35</sup> Winkler et al<sup>4</sup>, Bahat et al<sup>12</sup> and Goodacre et al<sup>13</sup> reported the unfavorable survival rate of short implants compared to regular implants. For those studies, short implants used were mainly machined surface external hexagon design or hydroxyapatite-coated cylinder design.<sup>4,12,13</sup> Unlike the present study that used the tapered crest module, rough surface, plateau design which similar to the optimized implant design by Shi et al. This may result in the different load transfer characteristics of implants leading to the different survival rates.

For this study, a cone beam computed tomography scan was not used to derive the bone models. Rather, these bone models were computer-generated. However, when compared to the study by Shi et al, similar trends were found for the Von Mises stresses at the bone-implant interface.<sup>34</sup> This present study showed that stresses concentrated on the implant crest module and continuously reduced along the sloping shoulder. Also, short implants showed the higher Von Mises stresses at the crestal region compared to regular implants as shown in Figure 19.

Of the loading conditions selected, the 15-degree angle oblique loads of 100 and 200 N were chosen to be tested because these forces were comparable to in vivo forces of mastication. These forces are biologically feasible actions that can be performed on an implant in vivo.<sup>44,45</sup> Oblique loads represent a more realistic scenario of mastication than forces applied only in the occlusal directions. For a given force, oblique forces will cause the highest localized stress in the cortical bone.<sup>24</sup> In fact, under static force measurements, Helkimo et al. indicated that the average biting force is 100-150 N in adult males, who have a higher biting force than females.<sup>45</sup>

Shulte et al. measured the C/I ratio of single tooth implant-supported restorations with a survival rate of 98.2 % and reported a mean C/I ratio of 1.3/1, which is similar to that of Model A.<sup>21</sup> Moreover, Blanes et al. conducted a longitudinal prospective study on the influence of C/I ratio on crestal bone loss around dental implants placed in the posterior region.<sup>19</sup> The mean clinical C/I ratio was 1.77 and the cumulative survival rate of implants with a C/I ratio equal to or greater than 2 was 94.1%. Higher C/I ratios were associated with less crestal bone loss. In a recent radiographic study by Birdi et al., the C/I ratio of single implant-supported restorations on short-length plateau-design implants in a clinical practice had a mean value of 2.0.<sup>22</sup> The average mesial and distal first bone-to-implant contact levels were 0.2 and 0.2 mm, respectively. It was concluded that the C/I ratio did not affect the success of the short-length plateau-design implants. In this study, mean age of patients was 61.3. Interestingly, occlusal forces are somewhat decreased due to age-related deterioration of the dentition in most situations.<sup>45</sup> In Birdi's study, the population of patients involved implant placement in posterior region.<sup>22</sup> The 93.2 % of implant sites were in the posterior region, which resulted in 60.5 % of tooth replaced were molars.<sup>22</sup> Location of an implant in the arch is directly related to the direction of forces. In the posterior region, the directions of forces are more vertical compared to the anterior region, which has more oblique forces. Based on the findings in this study under vertical loads of 100, 200 and 700 N, all implant models showed peak stress values far below the physiological limit of bone. This simulation may be approximated to the occlusal forces generated in the molar region, which is more vertical. Thus, location of an implant in the arch is an important factor to be considered when using short implants.

At normal masticatory forces (100 and 200 N), the use of short implants with the disproportionate C/I ratios showed the peak tensile and compressive stress values below the physiological limits of cortical and trabecular bone. The results from the present simulations may indicate that a disproportionate C/I ratio under normal masticatory forces does not affect implant survival rate as also shown clinically by Schulte et al<sup>21</sup>, Blanes et al<sup>19</sup>, and Birdi et al<sup>22</sup>'s studies. However, under overload conditions, increasing crown height increased the peak tensile and compressive stresses on the cortical bone. This increase in restoration height led to stress levels surpassing the threshold of physiological tolerance of cortical (100-190 MPa) and trabecular bone (5 MPa), which may lead to eventual failure of said bone.

Biomechanically, extending crown height increases force lever arm and results in higher compressive stresses as shown in Table 1. The results by Kitamura et al. showed that implants with pronounced crestal bone resorption around implant neck, which increased crown height demonstrated higher stresses.<sup>18</sup> Based on the findings of this study, increasing length of implant and reducing C/I ratio decreased both peak tensile and compressive stresses.

One interesting finding was that short implants (Model A and B) were associated with higher tensile stresses regardless of loading conditions and abutment heights. For vertical loads, short implants demonstrated higher tensile stresses compared to regular implants. Increasing implant length from 6 mm to 11 mm reduced peak tensile stresses by 53.28 % under vertical loads of 700 N. Sahin et al. stated multiple factors influencing load distribution on implants, such as gender, age, location of implant in the arch and parafunctional habits.<sup>25</sup> In patients with parafunctional habits or those with high stress

factors, implant length may play a more important role to the survival rate compared to implants placed in patients with normal masticatory forces.<sup>9</sup>

Bates et al described the nature of mastication as a chewing cycle.<sup>48</sup> The average human chewing frequency is 75 strokes/min. The duration of tooth contact in 1 cycle is about 0.3 seconds. It is the repetition of loadings. The present simulation was performed with static loadings while occlusal loading is cyclic in nature. As the number of cycles of load increases, forces required to induce bone failure may be less than the static loads that were tested in this present study.

Due to the complexity of three-dimensional implant modeling, short implants produced from only one manufacturer were included in the study. The same simulation may be used to compare stress distribution patterns among different commercial implants.

**Conclusion.**

Within the limitations of this study, the stress distribution patterns under oblique loads of 100 and 200 N were similar in all models regardless of the C/I ratio. The peak compressive and tensile stresses on the cortical and trabecular bone were below the physiological tolerance, even though implants with 2/1 C/I ratios produced higher stresses.

At 700 N, increasing crown height as in Model B resulted in the peak tensile and compressive stresses exceeding the physiological limits, which may lead to bone failure. Increasing implant length reduced the peak tensile and compressive stresses as seen in other models.

Stress distribution patterns for pure vertical loads of 100, 200, and 700 N were similar in all models regardless of the C/I ratio. The peak compressive and tensile stresses on the cortical and trabecular bone were below the physiological tolerance for all pure vertical load levels.

**Clinical implication**

In a normal masticatory environment, short implants may function under the physiological tolerance of bone. However, disproportionate C/I ratio may lead to bone failure under overload conditions.

## Bibliography

1. Adell R, Lekholm U, Rockler B, Brånemark PI. A 15-year study of osseointegrated implants in the treatment of the edentulous jaw. *Int J Oral Surg* 1981;10:387-416.
2. Zarb GA, Schmitt A. The longitudinal clinical effectiveness of osseointegrated dental implants: the Toronto study. Part III: Problems and complications encountered. *J Prosthet Dent* 1990;64:185-94.
3. Cooper LF. A role for surface topography in creating and maintaining bone at titanium endosseous implants. *J Prosthet Dent* 2000;84:522-34.
4. Winkler S, Morris HF, Ochi S. Implant survival to 36 months as related to length and diameter. *Ann Periodontol* 2000;5:22-31.
5. Lee JH, Frias V, Lee KW, Wright RF. Effect of implant size and shape on implant success rates: a literature review. *J Prosthet Dent* 2005;94:377-81.
6. Krogh PH, Worthington P, Davis WH, Keller EE. Does the risk of complication make transpositioning the inferior alveolar nerve in conjunction with implant placement a "last resort" surgical procedure? *Int J Oral Maxillofac Implants* 1994;9:249-54.
7. Renouard F, Nisand D. Impact of implant length and diameter on survival rates. *Clin Oral Implants Res* 2006;17:35-51.
8. Kotsovilis S, Fourmoussis I, Karoussis IK, Bamia C. A systematic review and meta-analysis on the effect of implant length on the survival of rough-surface dental implants. *J Periodontol* 2009;80:1700-18.
9. Misch CE. *Contemporary Implant Dentistry*. 3<sup>rd</sup> ed. St. Louis: Elsevier; 2008. p. 105-129,543-556.
10. Van Staden RC, Guan H, Loo YC. Application of the finite element method in dental implant research. *Comput Methods Biomech Biomed Engin* 2006;9:257-70.
11. Hagi D, Deporter DA, Pilliar RM, Arenovich T. A targeted review of study outcomes with short (< or = 7 mm) endosseous dental implants placed in partially edentulous patients. *J Periodontol* 2004;75:798-804.
12. Bahat O. Brånemark system implants in the posterior maxilla: clinical study of

- 660 implants followed for 5 to 12 years. *Int J Oral Maxillofac Implants* 2000;15:646-53.
13. Goodacre CJ, Kan JY, Rungcharassaeng K. Clinical complications of osseointegrated implants. *J Prosthet Dent* 1999;81:537-52.
  14. Scurria MS, Morgan ZV 4th, Guckes AD, Li S, Koch G. Prognostic variables associated with implant failure: a retrospective effectiveness study. *Int J Oral Maxillofac Implants* 1998;13:400-6.
  15. Grant BT, Pancko FX, Kraut RA. Outcomes of placing short dental implants in the posterior mandible: a retrospective study of 124 cases. *J Oral Maxillofac Surg* 2009;67:713-7.
  16. Romeo E, Bivio A, Mosca D, Scanferla M, Ghisolfi M, Storelli S. The use of short dental implants in clinical practice: literature review. *Minerva Stomatol* 2010;59:23-31
  17. Anitua E, Tapia R, Luzuriaga F, Orive G. Influence of implant length, diameter, and geometry on stress distribution: A finite element analysis *Int J Periodontics Restorative Dent* 2010;30:88-95.
  18. Kitamura E, Stegaroiu R, Nomura S, Miyakawa O. Biomechanical aspects of marginal bone resorption around osseointegrated implants: considerations based on a three-dimensional finite element analysis. *Clin Oral Impl Res* 2004;15:401-12.
  19. Blanes RJ, Bernard JP, Blanes ZM, Belser UC. A 10-year prospective study of ITI dental implants placed in the posterior region. II: Influence of the crown-to-implant ratio and different prosthetic treatment modalities on crestal bone loss. *Clin Oral Implants Res* 2007;18:707-14.
  20. Blanes RJ. To what extent does the crown-implant ratio affect the survival and complications of implant-supported reconstructions? A systematic review. *Clin Oral Impl Res* 2009;20:67-72.
  21. Schulte J, Flores AM, Weed M. Crown-to-implant ratios of single tooth implant-supported restorations. *J Prosthet Dent* 2007;98:1-5.
  22. Birdi B, Schulte J, Kovacs A, Weed M, Chuang SK. Crown-to-implant ratios of short-length implants. *J Oral Implantol* 2010, In-Press.
  23. Skalak R. Biomechanical considerations in osseointegrated prostheses. *J Prosthet Dent* 1983;49:843-8.

24. Geng JP, Tan KB, Liu GR. Application of finite element analysis in implant dentistry: a review of the literature. *J Prosthet Dent* 2001;85:585-98.
25. Sahin S, Cehreli MC, Yalçın E. The influence of functional forces on the biomechanics of implant-supported prostheses: a review. *J Dent*. 2002;30:271-82.
26. Smith DE, Zarb GA. Criteria for success of osseointegrated endosseous implants. *J Prosthet Dent* 1989;62:567-72.
27. Brånemark PI, Hansson BO, Adell R, Breine U, Lindström J, Hallén O, Ohman A. Osseointegrated implants in the treatment of the edentulous jaw. Experience from a 10-year period. *Scand J Plast Reconstr Surg Suppl* 1977;16:1-132.
28. Albrektsson T, Zarb G, Worthington P, Eriksson AR. The long-term efficacy of currently used dental implants: a review and proposed criteria of success. *Int J Oral Maxillofac Implants* 1986;1:11-25.
29. Chun HJ, Shin HS, Han CH, Lee SH. Influence of implant abutment type on stress distribution in bone under various loading conditions using finite element analysis. *Int J Oral Maxillofac Implants* 2006;21:195-202.
30. Kitagawa T, Tanimoto Y, Odaki M, Nemoto K, Aida M. Influence of implant/abutment joint designs on abutment screw loosening in a dental implant system. *J Biomed Mater Res B Appl Biomater* 2005;75:457-63.
31. Quaresma SE, Cury PR, Sendyk WR, Sendyk C. A finite element analysis of two different dental implants: stress distribution in the prosthesis, abutment, implant, and supporting bone. *J Oral Implantol* 2008;34:1-6.
32. Maeda Y, Miura J, Taki I, Sogo M. Biomechanical analysis on platform switching: is there any biomechanical rationale? *Clin Oral Implants Res* 2007;18:581-4.
33. Tabata LF, Assunção WG, Adelino Ricardo Barão V, de Sousa EA, Gomes EA, Delben JA. Implant platform switching: biomechanical approach using two-dimensional finite element analysis. *J Craniofac Surg* 2010;21:182-7.
34. Shi L, Li H, Fok AS, Ucer C, Devlin H, Horner K. Shape optimization of dental implants. *Int J Oral Maxillofac Implants* 2007;22:911-20.

35. Bozkaya D, Muftu S, Muftu A. Evaluation of load transfer characteristics of five different implants in compact bone at different load levels by finite elements analysis. *J Prosthet Dent* 2004;92:523-30.
36. Chun HJ, Cheong SY, Han JH, Heo SJ, Chung JP, Rhyu IC, Choi YC, Baik HK, Ku Y, Kim MH. Evaluation of design parameters of osseointegrated dental implants using finite element analysis. *J Oral Rehabil* 2002;29:565-74.
37. Huang HL, Chang CH, Hsu JT, Fallgatter AM, Ko CC. Comparison of implant body designs and threaded designs of dental implants: A 3-dimensional finite element analysis. *Int J Oral Maxillofac Implants* 2007;22:551-62.
38. Li T, Kong L, Wang Y, Hu K, Song L, Liu B et al. Selection of optimal dental implant diameter and length in type IV bone: a three dimensional finite element analysis. *Int J Oral Maxillofac Surg* 2009;38:1077-83.
39. Ding X, Liao SH, Zhu XH, Zhang XH, Zhang L. Effect of diameter and length on stress distribution of the alveolar crest around immediate loading implants. *Clin Implant Dent Relat Res* 2008;11:279-87.
40. Baggi L, Cappelloni I, Girolamo MD, Maceri F, Variro G, The influence of implant diameter and length on stress distribution of osseointegrated implants related to crestal bone geometry: A three dimensional finite element analysis. *J Prosthet Dent* 2008;100:422-31.
41. Petrie CS, Williams JL. Comparative evaluation of implant designs: influence of diameter, length, and taper on strains in the alveolar crest: A three-dimensional finite element analysis. *Clin Oral Impl Res* 2005;16:486-94.
42. Jokstad A, Braegger U, Brunski JB, Carr AB, Naert I, Wennerberg A. Quality of dental implants. *Int Dent J* 2003;53:409-43.
43. Lekholm U, Zarb GA: Patient selection and preparation. In: Brånemark PI, Zarb GA, Albrektsson T (eds): *Tissue-integrated prostheses: Osseointegration in clinical dentistry*. Quintessence, Chicago 1985, pp 199-209
44. Schrotengoer J, Tsao YP, Kinariwala V, Wang HM. Effect of microthreads and platform switching on crestal bone stress levels: A finite element analysis. *J Periodontol* 2008;79:2166-72.
45. Helkimo E, Carlsson GE, Helkimo M. Bite force and state of dentition. *Acta Odontol Scand*. 1977;35:297-303.

46. Borchers L, Reichart P. Three-dimensional stress distribution around a dental implant at different stages of interface development. *J Dent Res* 1983;62:155-9.
47. Gibbs CH, Mahan PE, Mauderli A, Lundeen HC, Walsh EK. Limits of human bite strength. *J Prosthet Dent* 1986;56:226-9.
48. Bates JF, Stafford GD, Harrison A. Masticatory function--a review of the literature. 1. The form of the masticatory cycle. *J Oral Rehabil* 1975;2:281-301.